

A Patternless Piezoelectric Energy Harvester for Ultra Low Frequency Applications

M. R. Awal^{1*}, M. Jusoh², T. Sabapathy², R. B. Ahmad², M. R. Kamarudin³, M. N. Osman², M F. Ahmad¹, S. A. Rahman¹, A. N. Dagang¹

¹Faculty of Ocean Engineering, Technology and Informatics,
Universiti Malaysia Terengganu (UMT), Kuala Nerus, Terengganu, 21030, MALAYSIA

²BioEM, School of Computer and Communication Engineering,
Universiti Malaysia Perlis (UniMAP), Kampus Pauh Putra, Arau, Perlis, 02600, MALAYSIA

³Faculty of Electrical and Electronic Engineering,
Universiti Tun Hussein Onn Malaysia, Parit Raja, Johor, 86400, MALAYSIA

DOI: <https://doi.org/10.30880/ijie.2020.12.07.021>

Received 3 September 2020; Accepted 12 October 2020; Available online 31 October 2020

Abstract: This paper presents a pattern less piezoelectric harvester for ultra low power energy applications. Usually patterned cantilevers are used as vibration energy harvester which results additional fabrication process. Hence, to reduce the process, a four layer cantilever configuration is used to design the harvester with Aluminum, Silicon and Zinc Oxide. The device dimension is settled to $12 \times 10 \times \approx 0.5009 \text{ mm}^3$ with $\approx 300 \text{ nm}$ deposition thickness for each layer. The modeling and fabrication processes are demonstrated in detail. The induced voltage by the cantilever is obtained through the analytical and practical measurements. From the measurements, it is found that, the maximum induced voltage is 91.2 mV from practical measurement with voltage density of 1.517 mV/mm^3 . It is evident from the results that, this pattern less model can be useful for next generation vibration energy harvester with simpler technology.

Keywords: Piezoelectric harvester, Vibration energy, Ultra low frequency energy, Multilayer cantilever

1. Introduction

Wireless devices have drawn the commercial attention and become the trend of modern technologies recently. With enormous potential, the major advantage of these devices is the ease of storage platform, i.e., the device does not rely on the storage to function. As a potential, the portable or embedded batteries can be removed from the system entirely by wireless energy harvesting technology [1, 2]. Now, wireless energy harvesting for low power applications can be achieved either by using a stationary energy source or harvesting ambient energy. For the latter case, available ambient energy is harvested and delivered to the application. To do so, electrostatic, thermal, piezoelectric and magnetic strategies are the mostly practiced methods [3]. More specifically, piezoelectric (to harvest vibration and acoustic energy) is more advantageous due to the broad material availability [4, 5].

To harvest the vibration energy, circular shaped piezoelectric cantilevers are practiced widely. However, the rectangular cantilever model can be adventurous for high pressure medium [6, 7]. Among rectangular shape, both patterned and pattern less cantilever are available [8]. However, pattern less cantilever, which is composed of simple sandwiched layers are very particular. These devices have the simplest form of configuration, as they only have electrode, base and energy harvesting layers. Also, no pattern (i.e. zigzag, curved, spring shape) is available on the device. Hence, it requires fewer and less complex fabrication steps which results financial benefits [9, 10].

From these motivations, we propose a cantilever based piezoelectric vibration energy harvester for ultra low frequency in this paper. We have considered less than 40 Hz, more precisely, 1 - 40 Hz as ultra low frequency. The

*Corresponding author: rabiulawall@gmail.com

cantilever model is designed by following a four layer configuration using Aluminum and Zinc Oxide with the Silicon base. Zinc Oxide (ZnO) is used for the piezoelectric layer. Top and bottom electrode layers are developed by Aluminum. The base layer is confirmed by Silicon and the thickness is settled to ≈ 0.5 mm whereas all other 3 layers have ≈ 0.0003 mm thickness each. The length and width of the cantilever is 12 mm and 10 mm respectively. Hence, the total device size is approximately $12 \times 10 \times 0.5009$ mm³.

The rest of this paper is distributed as follows; section 2 presents an analytical model for the cantilever. In the following section, the design and fabrication process of the cantilever are described in detail with the device performances. The performance is considered in the context of induced voltage. Lastly, the paper is concluded with some prospective future agendas.

2. Governing Equations

2.1 Force voltage relationship

An analytical proposal is developed by classical unimorph cantilever model. The model is a base clamped rectangular cantilever and has four layers configuration. The layers include two electrode layers, one piezoelectric layer and a base layer, as depicted in Fig. 1(a). A force can be applied on the cantilever which causes an induced voltage in the piezoelectric layer. We can describe the model in terms of induced voltage against an applied force, as equation (1) and (2). To describe the model, let us consider a force, F is applied on a base clamped rectangular cantilever. Then, the induced voltage, E can be defined as [11],

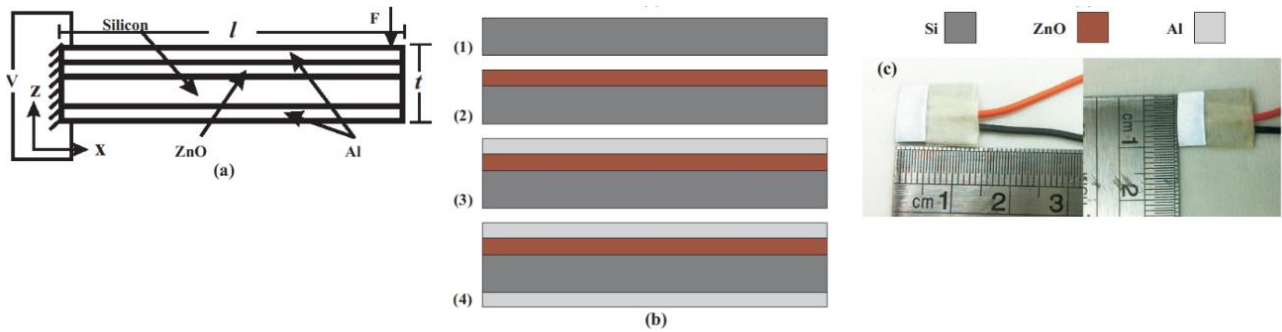


Fig. 1 - Proposed cantilever (a) classical descriptions, (b) fabrication process of cantilever beam, (c) fabricated cantilever ($12 \times 10 \times 0.5009$ mm³)

$$E = \frac{NF}{[1 - \omega^2 M C_m]} \tag{1}$$

Where,

$$N = \left[\frac{3g_{31}l}{8\omega t} \right] \tag{2}$$

And

$$C_m = \frac{4l^3}{Y_{11}^D \omega t^3} \tag{3}$$

$$M = \left(\frac{24}{\pi^4} \right) \rho l \omega t \tag{4}$$

Here, N (in v/n) is the transducer ratio, C_m (in m/n) is the compliance and M (in kg) is the effective mass of the cantilever. Yielding for a four layers configuration results,

$$E = \left(\frac{3}{8} \right) \left[\frac{F g_{31} \pi^4 Y_{11}^D l t}{\omega (\pi^4 t^2 Y_{11}^D - 96 \omega^2 l^4 \rho)} \right] \tag{5}$$

Where, g_{31} is the piezoelectric constant (V-m/N), ρ is the density of the material, Y_{11}^D represents Young's modulus of the materials. l , w and t are the length, width and total thickness of the cantilever, respectively. Total thickness can be expressed in terms of the layer thickness of ZnO, Al and Si as,

$$t = t_{ZnO} + 2t_{Al} + t_{Si} \quad (6)$$

The resonant frequency, F_r of a rectangular cantilever can be expressed by,

$$F_r = \frac{e_n^2}{2\pi l^2} \sqrt{\frac{Y_{11}^D t^2}{12\rho}} \quad (7)$$

Where, e_n is the Eigen value of n-th mode which is 1.875 for the fundamental mode of the cantilever. It is noticeable from the equation (7) that, the length of the cantilever has the inverse relationship with the resonant frequency. Hence, smaller length results larger frequency.

3. Cantilever Fabrication Process

Based on the analytical results, we have developed the rectangular cantilever by depositing layers using electron beam physical vapor deposition (EBPVD) machine. There are several materials to choose for the piezoelectric layer from the potential list [12, 14]. Among them, Lead Zirconate Titanate is being used most frequently. However, it is not environment friendly as it contains lead. Additionally, it is strongly affected by the temperatures and cannot be used for long duration due to the mechanical properties. In the alternatives, Zinc Oxide (ZnO) and Aluminum Nitride (AlN) are found as the active piezoelectric material, which do not contain lead. Hence, they are relatively more bio-compatible [15]. However, ZnO is more available with comparatively lower cost with longer life cycle. Again, ZnO has better voltage coefficient which implies better output against an applied stress, in terms of volts [16]. Reasonably, we are provoked to consider ZnO as the deposition material. ZnO pellet is used as the deposit for the target layer. The pellet is selected from the industrial grade granule white ZnO. The physical descriptions of the cantilever are presented in Table 1.

Table 1 - Parametric device descriptions

Parameter	Values	Symbol	Unit
<i>Cantilever</i>			
Length	12	l	mm
Width	10	w	mm
Thickness	≈ 0.5009	t	mm
<i>Layer thickness</i>			
ZnO	≈ 0.0003	t_{ZnO}	mm
Al	$\approx 2 \times 0.0003$	t_{Al}	mm
Base Si	≈ 0.5	t_{Si}	mm
<i>Density</i>			
ZnO	5.606	ρ_{ZnO}	g/cm^3
Silicon	2.333	ρ_{Si}	g/cm^3
Aluminum	2.700	ρ_{Al}	g/cm^3
<i>Young's modulus</i>			
piezoelectric [13]	40	Y_{11}^D	GPa
Si wafer	163		GPa
Al	69		GPa
<i>Poisson's ratio</i>			
Si wafer	0.27		
ZnO	0.39		
Al	0.334		
Piezoelectric constant	-9	g_{31}	$V-m/N$

3.1 Cantilever layer deposition

The proposed and fabricated cantilever is presented in Fig. 1(a) and 1(c). The consequent layer descriptions are depicted in 1(b). From the figures we can see, the cantilever has four layer configuration. The base platform of the cantilever is the silicon wafer, on which the piezoelectric layer is deposited. The silicon wafer is sliced from a commercial grade 100 mm N-type silicon wafer disk. The disk is one side polished and has 0.525 mm initial thickness. Top and bottom electrodes are deposited accordingly over the piezoelectric layer and beneath the silicon platform. Aluminum is selected as the electrode deposition material. The electrode layers are selected as flat pattern similar to the piezoelectric layer in length and width.

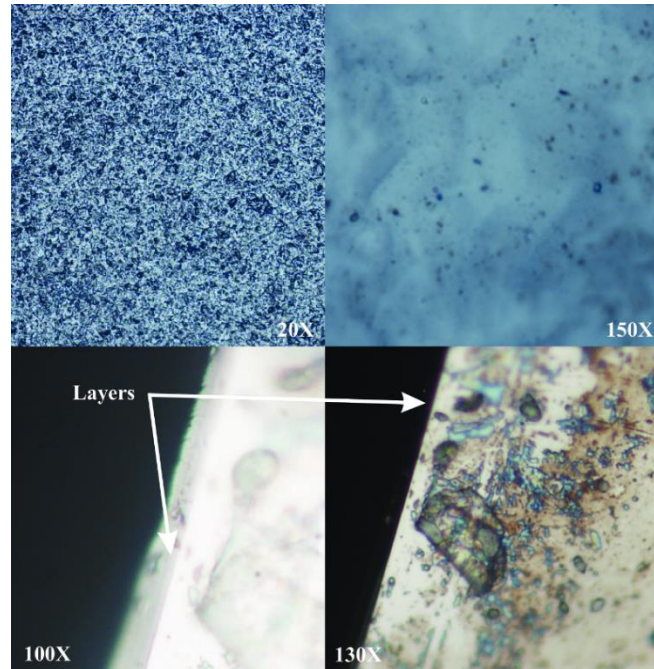


Fig. 2 - Microscopic photograph of the deposition layers, deposited aluminum surface (top), ZnO and Al layers of the cantilever (bottom)

The fabrication takes four steps to complete as follows,

1. Etching
2. ZnO deposition
3. Top electrode deposition and
4. Bottom electrode deposition

Firstly, the sliced wafer block is prepared for deposition by initial cleaning and etching. Potassium hydroxide (KOH) is used for the thickness etching from ≈ 0.525 mm to approximately 0.500 mm. The wafer is then ready to be deposited with the desired materials. The layer of ZnO is deposited by the EBPVD machine in the next step. After that, the model undergoes for the thickness and layer inspections by atomic-force microscopy (AFM) and thickness meter. The deposited ZnO layer has the thickness of approximately 300 nm.

In the following steps, the Al layers are deposited and confirms the top and bottom electrodes with ≈ 300 nm of thickness for each layer. Again, another round of thickness and layer inspections are performed. Lastly, the prototype is checked for any external damage. These whole deposition steps are performed in the room temperature. The details are depicted in Fig. 1(b). The microscopic images are presented in Fig. 2.

3.2 Experimental Setup and Tests

We have performed three tests to evaluate the performance of the cantilever in ultra low frequency. One with a programmed shaker as shown in Fig. 3. In other two tests, the cantilever is mounted on a motor bike and a car, in both running and parked mode. The results are shown in Fig. 5 (a) and 5 (b). The details are given in the following discussions. In the first test, we have applied a range of programmed force on the cantilever and read the consequent output. The force applied is ranged from minimum 10 g to maximum 120 g, which are equivalent to 0.098 N to 1.17 N. Fig. 4 (a) shows the relationship between the induced voltage and the applied force, for both the theoretical and measured values. We have observed the effective output achieved from different position of force from the clamped base of the cantilever. It is

worthy to point that, the force applied on the tip of the cantilever has benefited the output with maximum values. Hence, we are presenting the force applied on the device tip only.

We have added the road test to extend our experience in the ultra low frequency real environment with the proposal. To do so, we have mounted the cantilever on a motor bike and later on a car. Then, we have recorded the vibration responses while the vehicles are in parking and running mode. In parking mode, the vehicle is not moving but the engine was turned on. The vehicles were driven at less than 25 km/hr in running mode. Fig. 3 shows the test road for running mode. We have chosen the road due to the availability of road cracks and the bumps, as it tests the stability of the device. As mentioned earlier, Fig. 5 (a) and 5 (b) are showing the device output in terms of the induced voltages.



Fig. 3 - Experimental setup (Indoor and outdoor Test Road)

4. Performance Analysis of The Cantilever

4.1 Numerical analysis and indoor tests

The theoretical values are calculated by applying equation (2) while the measured data are achieved by performing actual force. In theory, the voltage can be as high as 9.04 mV with maximum applied force and as low as 0.94 mV with the minimum force, respectively. Practically, the maximum voltage is induced when 1.17 N force is applied, which is 8.7 mV. However, the increment of the output is not smoothly linear which lies within the values of 0.5 mV to 8.7 mV. Again, the difference between the theoretical and practical measurement is caused by the not perfect device fabrication.

To extend our observation, we have tested the device with very low frequency ranged from (1 Hz – 40 Hz) to trace the energy potential. We have used a programmed shaker as depicted in Fig. 3 which varies the shaking frequencies from 1 Hz to 40 Hz. We have increased the shaking frequency by 5 Hz in each step. The cantilever was shaken under open load mode. One end of the cantilever was attached with the shaker as depicted in Fig. 3. The obtained results are summarized in Fig. 4 (a) and 4 (b). From the Figures, we can see that, maximum 10.21 mV output is found when the maximum frequency of 40 Hz is applied. Again, the minimum output is found from applied frequency of 1 Hz for free load mode which is expected. It is noticeable that, the development of the output is linear to the progression of the applied frequency, i.e. higher the frequency, higher the output.

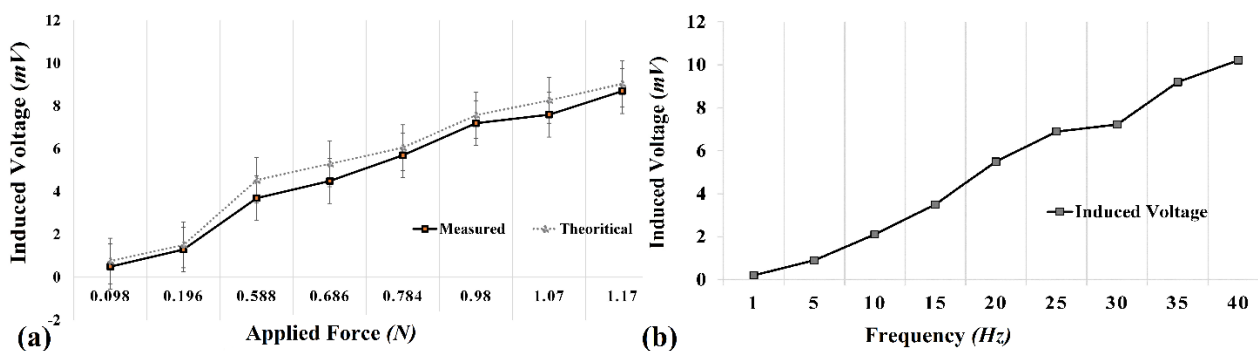


Fig. 4 - (a) Induced voltage vs. applied force, (b) Induced voltage vs. applied frequency

It is evident from the results that, the cantilever did not achieve the output of its resonant frequency with the applied force. We can apply equation (7) to find the resonant frequency. According to the equation, the resonant frequency of the cantilever is 345.0434 Hz. Hence, it is unexpected to achieve that in less than 50 Hz applied frequency.

4.2 Under nonuniform force

The prototype was tested under high and nonuniform force ranged from 1 N to 19.61 N to evaluate its stability. We have applied maximum 2 kilograms or 19.61 N on the prototype. We have received the voltage response against the applied force. The responses are shown in table 2 and Fig. 6. From the table 2 and Fig. 6 we can trace that, the device produces linear responses against the nonuniform applied force. Maximum 91.2 mV is found from 19.61 N applied force. However, 40.1 mV output is found when 9.81 N or 1 kg force is applied.

4.3 Outdoor tests

Fig. 5 (a) and 5 (b) suggest that, maximum 7.8 mV is induced from the car and 6.7 mV from the motor bike in running mode. However, in parking mode, motor bike performs better with 4.7 mV induced voltage compared to 0.9 mV from the car.

Table 2 - Applied force response

Applied force (N)	Voltage response (mV)
9.81	40.1
11.77	51.2
14.71	65.6
16.67	72.3
19.61	91.2

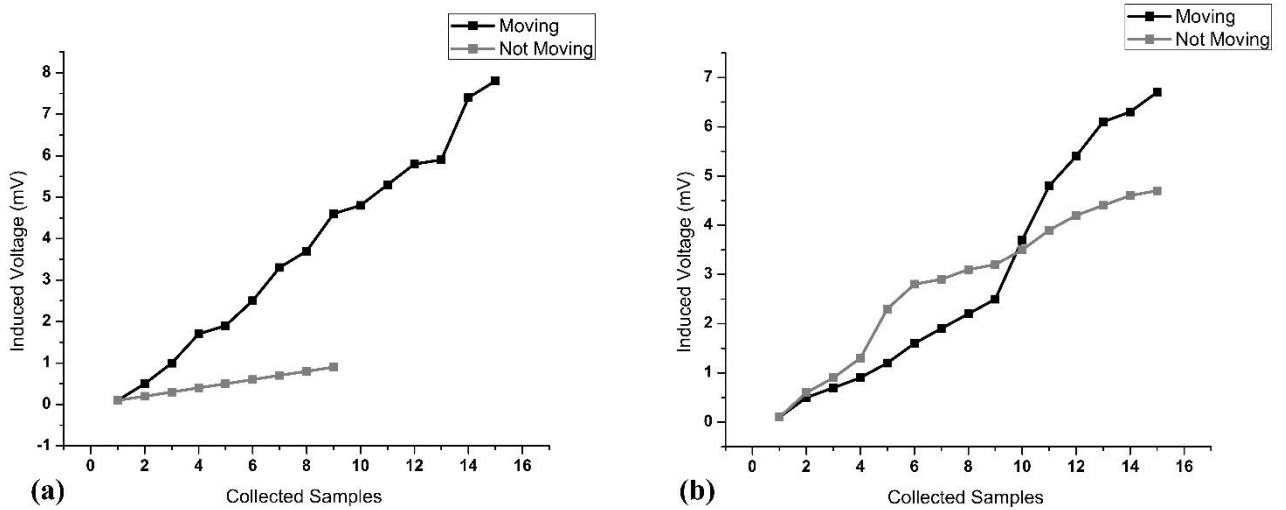


Fig. 5 – (a) Induced voltage vs. applied force, (b) Induced voltage vs. applied frequency

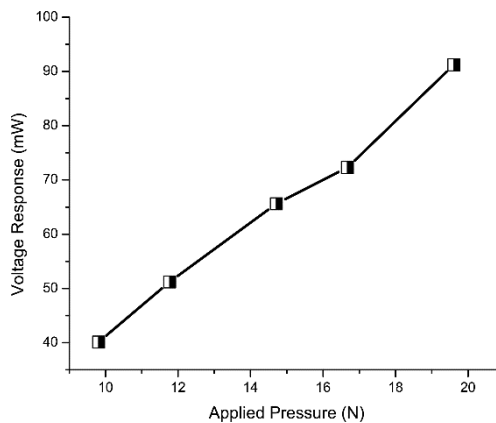


Fig. 6 - Voltage response under applied force

We have compared our proposed cantilever with several existing models. The summary is presented in table 3. From the table, it is quite clear that, this work results very competitive and optimal induced voltage density, if the design complexities are considered. This work is completed using the pattern less model, simplest fabrication process and available materials. Yet, compared to 16.43 and ≈ 1.535 mV/mm³ from [22] and [23], this work has achieved 1.517 mV/mm³. However, falls behind in the terms of induced voltage in <50 Hz. Nevertheless, some of them are not appropriate for force and vibration dual energy harvesting [22, 24]. Also, [20] requires higher force to achieve the mentioned performances. [25] requires the operating temperature to be above than the room temperature.

Again, most of the high performance models are very complicated to design, hence costly, even for the commercial production [22, 24, 19, 18]. [19] is not applicable for outdoor application due to the fragile configuration. [18] is one of the most appropriate energy harvester for ultra low frequencies. However, the fabrication process and cost are acting as the barrier for commercial production. [25] shows the moderate induced voltage with 290 mV. However, the fabrication complexity provides a significant bottleneck to the performance tradeoff. Again, [21] was another proposal for multidimensional energy harvesting with very high induced voltage. However, the device can harvest only the vibration energy, not both with force energy. Also, the device configuration pulls some drawbacks due to the additional stress from the attached pendulum.

Table 3 - Summary of device comparison

Reference	Induced Voltage in <50 Hz	Materials	Device Dimension	Voltage Density (mV/mm ³)
[21]	≈ 4.5 V	PZT-5H	115.25×5.28×0.45 mm ³	16.43
[22]	≈ 13 V	Hybrid Piezoelectric	≈ 8466.59 mm ³	≈ 1.535
This work	≈ 91.2 mV	ZnO	$\approx 12 \times 10 \times 0.5009$ mm ³	1.517
[24]	≈ 4.9 V	Piezoelectric	160×85×85 mm ³	4.238×10 ⁻³
[18]	280 mV	PZT Film	10 × 10 mm ²	2.8 (mv/ mm ²)
[25]	< 100 mV	ZnO Film	1 cm ²	1 (mv/ mm ²)
[16]	NA	PbZr0.52Ti0.48O3	0.6 mm ³	NA
[19]	NA	ZnO	500×100×0.3 μm ³	NA
[20]	NA	ZnO Film	50 × 50 mm ²	NA
[17]	0 mV	Piezoelectric	2039.68 mm ³	NA
[23]	NA	ZnO Film	14.5×14.5×0.5 mm ³	NA

The aforementioned discussions and presented data suggest that, the fabricated cantilever can harvest vibration energy under high force and very low frequencies. The used materials to construct the device are highly available at low cost. They are bio-compatible as well. At the same point, our proposal has met the optimized performance with very low cost and simple fabrication process. Again, as the cantilever is patternless, hence, the design of it is comparatively easy. In addition, the device fabrication requires only four steps to be completed and can be implemented for hybrid energy harvesting platforms [26].

5. Conclusions

An energy harvester based on piezoelectric cantilever is presented in this paper. The modeling of the device is described in detail with the analytical and experimental explanation. The fabrication of the device is discussed in detail. The validation of the proposal is presented by the force induced voltage. In addition, a range of frequencies (which are less than the resonant frequency) are applied to observe the impact under a free load mode. From the findings, it is obvious that, the proposed harvester can produce voltage as high as 91.2 mV with 19.61 N applied force. However, when shaken with prescribed frequencies, the induced voltage can be as high as 10.21 mV. Hence, it is evident that, the proposed device can sustain under high stress. Additionally, the device can harvest ultra low frequency (1 Hz - 40 Hz) vibration energy. Therefore, the proposal is highly suitable for vibration energy harvesting and can be beneficial in acoustic energy transfer and ambient vibration energy harvesting. Future research will focus on the application of this cantilever in underwater environments to harvest the ocean energy.

Acknowledgement

This work is partly supported by Universiti Malaysia Terengganu, under fundamental research grant scheme (FRGS 59604), Ministry of Higher Education, Government of Malaysia.

References

- [1] Wei, C., & Jing, X. (2017). A comprehensive review on vibration energy harvesting: Modelling and realization. *Renewable and Sustainable Energy Reviews*, 74, 1-18

- [2] Priya, S., Song, H. C., Zhou, Y., Varghese, R., Chopra, A., Kim, S. G., ... & Polcawich, R. G. (2019). A review on piezoelectric energy harvesting: materials, methods, and circuits. *Energy Harvesting and Systems*, 4(1), 3-39
- [3] Tang, W. C., Nguyen, T. C., & Howe, R. T. (1989, February). Laterally driven polysilicon resonant microstructures. In *IEEE Micro Electro Mechanical Systems,, Proceedings,'An Investigation of Micro Structures, Sensors, Actuators, Machines and Robots'* (pp. 53-59). IEEE
- [4] Motamedi, M. E. (2005). *MOEMS: Micro-opto-electro-mechanical Systems* (Vol. 126). SPIE press
- [5] Rugar, D., Stipe, B. C., Mamin, H. J., Yannoni, C. S., Stowe, T. D., Yasumura, K. Y., & Kenny, T. W. (2001). Adventures in attonewton force detection. *Applied Physics A*, 72(1), S3-S10
- [6] Barnett, S. B., Rott, H. D., ter Haar, G. R., Ziskin, M. C., & Maeda, K. (1997). The sensitivity of biological tissue to ultrasound. *Ultrasound in Medicine and Biology*, 23(6), 805-812
- [7] Li, X., Shih, W. Y., Aksay, I. A., & Shih, W. H. (1999). Electromechanical behavior of PZT - brass unimorphs. *Journal of the American Ceramic Society*, 82(7), 1733-1740
- [8] Cha, Y., & You, H. (2018, March). Energy harvesting from torsions of patterned piezoelectrics. In *Active and Passive Smart Structures and Integrated Systems XII* (Vol. 10595, p. 105950F). International Society for Optics and Photonics
- [9] Jeong, S., Cho, J. Y., Sung, T. H., & Yoo, H. H. (2017). Electromechanical modeling and power performance analysis of a piezoelectric energy harvester having an attached mass and a segmented piezoelectric layer. *Smart Materials and Structures*, 26(3), 035035
- [10] Banerjee, S., & Roy, S. (2018). A dimensionally reduced order piezoelectric energy harvester model. *Energy*, 148, 112-122
- [11] Germano, C. (1971). Flexure mode piezoelectric transducers. *IEEE Transactions on audio and electroacoustics*, 19(1), 6-12
- [12] Wang, P., Fu, Y., Yu, B., Zhao, Y., Xing, L., & Xue, X. (2015). Realizing room-temperature self-powered ethanol sensing of ZnO nanowire arrays by combining their piezoelectric, photoelectric and gas sensing characteristics. *Journal of Materials Chemistry A*, 3(7), 3529-3535
- [13] Hoffmann, S., Östlund, F., Michler, J., Fan, H. J., Zacharias, M., Christiansen, S. H., & Ballif, C. (2007). Fracture strength and Young's modulus of ZnO nanowires. *Nanotechnology*, 18(20), 205503.
- [14] Wang, P., & Du, H. (2015). ZnO thin film piezoelectric MEMS vibration energy harvesters with two piezoelectric elements for higher output performance. *Review of Scientific Instruments*, 86(7), 075002
- [15] Chaudhuri, D., Kundu, S., & Chatteraj, N. (2019). Design and analysis of MEMS based piezoelectric energy harvester for machine monitoring application. *Microsystem Technologies*, 25(4), 1437-1446
- [16] Tang, G., Liu, J. Q., Yang, B., Luo, J. B., Liu, H. S., Li, Y. G., ... & Sugiyama, S. (2012). Piezoelectric MEMS low-level vibration energy harvester with PMN-PT single crystal cantilever. *Electronics letters*, 48(13), 784-786
- [17] Guiffard, B., Guichon, Y., & Gundel, H. W. (2012). Commercial piezoelectric unimorph diaphragm as a magnetic energy harvester. *Electronics letters*, 48(19), 1196-1198
- [18] 18. Y. H. Do, W. S. Jung, M. G. Kang, C. Y. Kang, and S. J. Yoon. Preparation on transparent flexible piezoelectric energy harvester based on PZT films by laser lift-off process. *Sensors and Actuators A: Physical*, Vol. 200, pp. 51-55, 2013
- [19] Do, Y. H., Jung, W. S., Kang, M. G., Kang, C. Y., & Yoon, S. J. (2013). Preparation on transparent flexible piezoelectric energy harvester based on PZT films by laser lift-off process. *Sensors and Actuators A: Physical*, 200, 51-55
- [20] Qin, W., Li, T., Li, Y., Qiu, J., Ma, X., Chen, X., ... & Zhang, W. (2016). A high power ZnO thin film piezoelectric generator. *Applied Surface Science*, 364, 670-675
- [21] Xu, J., & Tang, J. (2017). Modeling and analysis of piezoelectric cantilever-pendulum system for multi-directional energy harvesting. *Journal of Intelligent Material Systems and Structures*, 28(3), 323-338
- [22] Fan, K., Liu, S., Liu, H., Zhu, Y., Wang, W., & Zhang, D. (2018). Scavenging energy from ultra-low frequency mechanical excitations through a bi-directional hybrid energy harvester. *Applied Energy*, 216, 8-20
- [23] Tao, K., Yi, H., Tang, L., Wu, J., Wang, P., Wang, N., ... & Chang, H. (2019). Piezoelectric ZnO thin films for 2DOF MEMS vibrational energy harvesting. *Surface and Coatings Technology*, 359, 289-295
- [24] Wu, Y., Qiu, J., Zhou, S., Ji, H., Chen, Y., & Li, S. (2018). A piezoelectric spring pendulum oscillator used for multi-directional and ultra-low frequency vibration energy harvesting. *Applied energy*, 231, 600-614
- [25] Zhang, X., Wang, P., Liu, X., Zhang, W., Zhong, Y., Zhao, H., ... & Amarasinghe, Y. W. R. (2019). Effect of post-annealing on microstructure and piezoelectric properties of ZnO thin film for triangular shaped vibration energy harvester. *Surface and Coatings Technology*, 361, 123-129
- [26] Awal, M. R., Jusoh, M., Sabapathy, T., Kamarudin, M. R., Rahim, H. A., & Abd Malek, M. F. (2016, April). Analysis of a hybrid wireless power harvester for low power applications. In *2016 10th European Conference on Antennas and Propagation (EuCAP)* (pp. 1-5). IEEE